

# Solvent-resistant antibacterial microfibers of self-quaternized block copolymers from atom transfer radical polymerization and electrospinning

Fu Guo-Dong,\* Yao Fang, Li Zhigang and Li Xinsong

Received 18th October 2007, Accepted 3rd January 2008

First published as an Advance Article on the web 17th January 2008

DOI: 10.1039/b716127a

Diblock copolymers with one block of poly[[(2-dimethylamino)ethyl methacrylate)-*co*-(glycidyl methacrylate)] P(DMAEMA-*c*-GMA) and another of poly(pentachlorophenyl acrylate) (PPCPA) (P(DMAEMA-*c*-GMA)-*b*-PPCPA) were synthesized *via* consecutive atom transfer radical polymerization (ATRP). Electrospinning of P(DMAEMA-*c*-GMA)-*b*-PPCPA from a solution in THF and DMF gave rise to microfibers with diameters in the range of 300 nm to 1.3  $\mu\text{m}$ . Solvent-resistant microfibers were obtained by the subsequent treatment with 1,6-hexanediamine. The quaternary ammonium salts (QASs) were generated *via* *N*-alkylation of tertiary amine groups of the P(DMAEMA-*c*-GMA) block by the chloro-aromatic compounds of the PPCPA block (or self-quaternization of P(DMAEMA-*c*-GMA)-*b*-PPCPA). Combination of the hydrophobic interaction of the PPCPA and the electrostatic interaction of QASs from the self-quaternization of P(DMAEMA-*c*-GMA)-*b*-PPCPA gives the resulting microfibers a high antibacterial activity. The antibacterial effect of the crosslinked microfibers was assayed with *Escherichia coli* and *Staphylococcus aureus* cultures. 95% *E. coli* and 97% *S. aureus* were killed after being contacted with 50 mg P(DMAEMA-*c*-GMA)-*b*-PPCPA microfibers in 10 min. The permanence of the antibacterial activity of the self-quaternized P(DMAEMA-*c*-GMA)-*b*-PPCPA microfibers was also demonstrated in repeated applications.

## 1. Introduction

Microfibers with antibacterial activities are of global interest for their potential applications in various areas, particularly in medical devices, health care, hygienic applications, water-treatment, and food packaging and storage.<sup>1–3</sup> Electrospinning is an attractive approach for preparing continuous fibers from micro-scale to sub-micrometer-scale due to its low cost, wide applicability of materials and high production rate.<sup>2</sup> Elemental silver and silver salts have been widely used as antibacterial agents in recent decades. Polymeric microfibers with silver particles<sup>4–8</sup> have been prepared by electrospinning and exhibited high antibacterial activity.

The application of antibacterial polymers has attracted much attention because they minimize the environmental problems accompanying low-molecular weight conventional disinfectants or antimicrobial agents, such as toxicity of residues of these agents after leaching into the environment.<sup>9</sup> Cationic polymers with quaternary ammonium salts (QASs) or biguanide groups exhibit good antimicrobial activities.<sup>10,11</sup> Microfibers containing QASs have been prepared by electrospinning and demonstrated antimicrobial activity.<sup>12–14</sup> Polymers containing QASs are generally prepared *via* *N*-alkylation of tertiary amine groups by alkyl halide having 4–12 carbons.<sup>10</sup> The slowly leaching of the alkyl halide molecules from polymers<sup>15</sup> in repeated applications not only reduces the antibacterial effect, but also causes pollution to the environment. Thus, the preparation of solvent-resistant and

environmentally stable antibacterial microfibers would be of interest to academic research and industrial applications alike.

Recent progress in controlled/living radical polymerization, especially in atom transfer radical polymerization (ATRP), has provided a powerful tool for preparing nearly monodispersed polymers with controllable molecular weight.<sup>16–18</sup> Well-defined and multi-functional polymer architectures can also be prepared *via* ATRP.<sup>19,20</sup> Pentachlorophenol and its sodium salts are primarily used as antimicrobial and antifungal agents to prevent the growth of algae, fungi and bacteria.<sup>21</sup> However, the application of pentachlorophenol and its derivatives is restricted because of their adverse effects on the health of ecosystems, wildlife and people.<sup>22</sup> In this work, block copolymers of poly[[(2-dimethylamino)ethyl methacrylate)-*co*-(glycidyl methacrylate)] P(DMAEMA-*c*-GMA) and poly(pentachlorophenyl acrylate) (PPCPA) (P(DMAEMA-*c*-GMA)-*b*-PPCPA) were synthesized *via* consecutive ATRPs. Electrospinning of P(DMAEMA-*c*-GMA)-*b*-PPCPA polymers from a solution in THF and DMF gave rise to microfibers with diameters in the range of 300 nm to 1.3  $\mu\text{m}$ . Solvent-resistant nanofibers were obtained by treatment of 1,6-hexanediamine to crosslink the epoxy groups of P(DMAEMA-*c*-GMA)-*b*-PPCPA. The quaternary ammonium salts (QASs) were generated *via* *N*-alkylation of tertiary amine groups of the P(DMAEMA-*c*-GMA) block by the chloro-aromatic compounds of the PPCPA block (self-quaternization of P(DMAEMA-*c*-GMA)-*b*-PPCPA). Combination of the hydrophobic interaction of the PPCPA polymers and the electrostatic interaction of QASs from the self-quaternization of P(DMAEMA-*c*-GMA)-*b*-PPCPA resulted in microfibers exhibiting high antibacterial activity.

School of Chemistry and Chemical Engineering, Southeast University, Jiangning District, Nanjing, Jiangsu, P.R. China, 211189. E-mail: fu7352@seu.edu.cn; Fax: +86-25-52090621; Tel: +86-25-52090625

## 2. Experimental

### 2.1. Materials

The monomers (2-dimethylamino)ethyl methacrylate (DMAEMA, 98%) and glycidyl methacrylate (GMA, 97%) were purchased from Acros Organic Co, of Geel, Belgium. They were used after removal of inhibitors in a ready-to-use disposable inhibitor-removal column (Aldrich Chemical Co.). Ethyl 2-bromoisobutyrate (EBB, 98%) and *N,N,N',N',N''*-pentamethyldiethylenetriamine (PMDETA, 99%) were purchased from Aldrich Chemical Co. and were used as received. Sodium pentachlorophenol (85%), acyloyl chloride (98%), CuBr (99%) and 1,6-hexanediamine (98%) were purchased from Shanghai Chemical Reagent Plant. Before use, sodium pentachlorophenol was purified by recrystallization in distilled water. *Escherichia coli* (*E. coli*, ATCC DH5a) and *Staphylococcus aureus* (*S. aureus*, Newman) were obtained from the American Type Culture Collection. High purified nitrogen was used in all reactions.

### 2.2. Synthesis of pentachlorophenyl acrylate (PCPA)

Sodium pentachlorophenol (5.8 g, 0.02 mol) and 40 ml of ethyl acetate were introduced into a 100 ml three-neck round-bottom flask equipped with a dropping funnel and a nitrogen inlet/outlet. After cooling to 0 °C, 1.8 ml of acyloyl chloride (0.022 mol) in 10 ml of ethyl acetate were added slowly, with continuous stirring, to the mixture over a period of 1 h under a nitrogen atmosphere. Then, the temperature was allowed to rise to room temperature. The reaction was run for another 4 h, and NaCl was removed from the mixture by filtration. The organic layer was washed with saturated brine solution several times until the pH reached about 7.0. The ethyl acetate layer was dried overnight with magnesium sulfate. After removal of the solvent by rotary evaporation, a white crystalline product was obtained. Yield: 70%; mp: 76 °C; <sup>1</sup>H NMR (DCCl<sub>3</sub>, δ/ppm): 163.0 (C=O), 143.8 (aromatic ring C–O), 135.5 (aromatic ring C–Cl), 130.6 (aromatic ring C–Cl), 133.2 (C=C), 127.3 (C=C). FTIR (solid, ATR cell): 176.19 (C=O), 1638.1 (C=C) cm<sup>-1</sup>.

### 2.3. Atom transfer radical polymerization

**2.3.1. Preparation of DMAEMA and GMA copolymers.** For a typical polymerization, 14.3 mg (0.1 mmol) of CuBr, 3.2 ml (19 mmol) of DMAEMA, 0.15 ml (1 mmol) of GMA and 1 ml of THF were introduced into a 25 ml glass tube. The reaction mixture was degassed by bubbling nitrogen through the solution for 20 min, then 17 μl (0.1 mmol) of EBB was added into the mixture under a nitrogen atmosphere. The reaction mixture was flushed with nitrogen for another 10 min. Finally, 21 μl (0.1 mmol) of PMDETA were added and the test-tube was fitted tightly with a rubber stopper under a nitrogen atmosphere. Polymerization was carried out under continuous stirring at 80 °C. After a predetermined period of time, the reaction was stopped and diluted with THF. The catalyst complex was removed from the reaction mixture by passing through an alumina column. The DMAEMA and GMA copolymer (P(DMAEMA-*c*-GMA)) was precipitated in an excess volume of petroleum ether. The resulting polymer was filtered and dried *in vacuo* overnight. About 1.8 g of white powders (yield ~ 55%,  $M_n = 1.7 \times 10^4$  g mol<sup>-1</sup>) were obtained.

**2.3.2. Preparation of P(DMAEMA-*c*-GMA)-*b*-PPCPA copolymer.** A dry Pyrex® test-tube equipped with a magnetic stirrer was charged with 0.85 g of P(DMAEMA-*c*-GMA) ( $M_n = 1.7 \times 10^4$  g mol<sup>-1</sup>), 1.5 g of PCPA and 3 ml of THF. The mixture was degassed by bubbling nitrogen through it for 15 min. After degassing, 7 mg (0.05 mmol) of CuBr was added carefully into the reaction mixture. The mixture was degassed by bubbling nitrogen through for another 15 min. Finally, 11 μl (0.05 mmol) of PMDETA was added and the test-tube was sealed under a nitrogen atmosphere with a rubber stopper. The reaction mixture was stirred at 70 °C for 4 h. The reaction mixture was then diluted with THF and passed through an alumina column to remove the metal complex. The resulting copolymer of P(DMAEMA-*c*-GMA)-*b*-PPCPA was precipitated in petroleum ether. After drying under reduced pressure overnight, about 1.3 g of white powders ( $M_n = 2.2 \times 10^4$  g mol<sup>-1</sup>) were obtained.

### 2.4. Electrospinning of P(DMAEMA-*c*-GMA)-*b*-PPCPA

P(DMAEMA-*c*-GMA)-*b*-PPCPA copolymer was dissolved in DMF–THF (volume ratio 2 : 3) to a concentration from 15 to 35% (g ml<sup>-1</sup>). In an electrospinning unit, the P(DMAEMA-*c*-GMA)-*b*-PPCPA solution was fed at a constant rate of 6 ml h<sup>-1</sup> to a syringe by a digitally controlled micropump. The tip of the syringe was connected to a high-voltage supply (Tianjing Dongwen High Voltage Electronics Inc.). Electrospinning was carried out at an electrical potential of 10 kV using a needle with an inner diameter of about 0.6 mm. The distance between the tip of the needle and the grounded collector was fixed at about 20 cm.

### 2.5. Crosslinking of the P(DMAEMA-*c*-GMA)-*b*-PPCPA microfibers

About 50 mg of P(DMAEMA-*c*-GMA)-*b*-PPCPA microfibers were immersed into a 5% of 1,6-hexanediamine solution in petroleum ether. The reaction was carried out at room temperature for about 2 h. Then, the crosslinked P(DMAEMA-*c*-GMA)-*b*-PPCPA microfibers were removed from the solution and rinsed with ethanol and distilled water thrice, respectively. The microfibers were dried under reduced pressure overnight.

### 2.6. Determination of antibacterial activity

Antibacterial efficiency tests were conducted using aqueous suspensions of *S. aureus* (or *E. coli*), which were cultivated in 50 ml of a 3.1% yeast–dextrose broth (containing 10 g l<sup>-1</sup> peptone, 8 g l<sup>-1</sup> beef extract, 5 g l<sup>-1</sup> sodium chloride, 5 g l<sup>-1</sup> glucose, and 3 g l<sup>-1</sup> yeast extract at a pH of 6.8)<sup>15</sup> at 37 °C. The *S. aureus* (or *E. coli*) concentration was estimated from the optical density at 540 nm, whereby the *S. aureus* (or *E. coli*) number was calculated based on the standard calibration that an optical density of 1.0 at 540 nm is equivalent to ~ 10<sup>9</sup> cells per ml.<sup>25</sup> All glassware and polymer samples were sterilized with UV irradiation before experiments.

The *S. aureus* (or *E. coli*) containing broth was centrifuged at 2700 rpm for 10 min. After removal of the supernatant, the *S. aureus* (or *E. coli*) cells were washed twice with a sterile phosphate buffer solution, PBS (containing 5.4 g of sodium dihydrogen phosphate monohydrate and 8.66 g of anhydrous disodium hydrogen phosphate in 1 l of distilled water, adjusted to pH 7.0),

and resuspended in PBS at a concentration of  $10^5$  cells  $\text{ml}^{-1}$ . About 50 mg of the P(DMAEMA-*c*-GMA)-*b*-PPCPA microfibers were introduced into 200 ml of the bacterial suspension in an Erlenmeyer flask. The flask was shaken at 200 rpm in a 37 °C bath. The P(DMAEMA-*c*-GMA)-*b*-PPCPA microfibers were presoaked in PBS (pH = 7.0) for 1 h, prior to immersion in the *S. aureus* (or *E. coli*) containing PBS, to ensure that they were thoroughly wetted. After the fiber had been in contact with the bacteria suspension for a prescribed period of time, 0.1 ml of the bacteria suspension was pipetted out from the flask and 0.9 ml of sterile water was added to this suspension. The suspension was diluted several times and 0.1 ml of the diluted suspension was spread onto a triplicate solid agar plate. The plates were then sealed and incubated at 37 °C for 24 h and the numbers of viable cells were counted. The results, after multiplication of the dilution factor, were expressed as the mean colony forming units per milliliter.

Antibacterial efficacy in repeated applications was investigated with 50 mg P(DMAEMA-*c*-GMA)-*b*-PPCPA microfibers. After one batch, microfibers were rinsed thrice with doubly distilled water and used for the next batch assay.

## 2.7. Characterization

The chemical structures of the P(DMAEMA-*c*-GMA) copolymers and P(DMAEMA-*c*-GMA)-*b*-PPCPA block copolymers were characterized by  $^1\text{H}$  and  $^{13}\text{C}$  NMR spectroscopy on a Bruker ARX 300 MHz spectrometer, using  $\text{CDCl}_3$  as the solvent in 1000 scans and a relaxation time of 2 s. Gel permeation chromatography (GPC) was performed on an HP 1100 high pressure liquid chromatograph (HPLC), equipped with an HP 1047A refractive index detector and a PLgel MIXED-C 300–7.5 mm column (packed with 5  $\mu\text{m}$  particles of different pore sizes). The column packing allowed the separation of polymers over a wide molecular weight range of 200–3 000 000. THF was used as the eluent at a low flow rate of 1  $\text{ml min}^{-1}$  at 35 °C. Polystyrene standards were used as the references. XPS measurements were carried out on a Kratos AXIS HSi spectrometer (Kratos Analytical Ltd, Manchester, England) with a monochromatized

Al  $K\alpha$  X-ray source (1486.6 eV photons). The X-ray source was run at a reduced power of 150 W (15 kV and 10 mA). The samples were mounted on standard sample studs by means of double-sided adhesive tape. The core-level spectra were obtained at the photoelectron take-off angle (with respect to the sample surface) of 90°. The pressure in the analysis chamber was maintained at  $10^{-8}$  Torr or lower during sample measurements. Surface elemental stoichiometries were determined from the spectral area ratios, after correcting with the experimentally determined sensitivity factors, and were reliable to within  $\pm 10\%$ . Scanning electron microscopy (SEM) measurements were carried out on an electron microscope (Hitachi X-650 SEM) at an accelerating voltage of 5–20 kV and an object distance of about 8 mm.

## 3. Results and discussion

### 3.1. Synthesis of P(DMAEMA-*c*-GMA)-*b*-PPCPA copolymers

Pentachlorophenyl acrylate (PCPA) can be polymerized *via* atom transfer radical polymerization (ATRP). However, the solubility of the PCPA polymer (PPCPA) is not very good in common solvents. Thus, in this work, copolymers of 2-(dimethylamino)ethyl methacrylate (DMAEMA) and glycidyl methacrylate (GMA) (P(DMAEMA-*c*-GMA)) were synthesized *via* ATRP and used as macroinitiators to prepare the block copolymer of P(DMAEMA-*c*-GMA) and PPCPA (P(DMAEMA-*c*-GMA)-*b*-PPCPA) (Fig. 1). In this work, GMA was introduced into the copolymer to prepare crosslinked microfibers *via* the reaction between the epoxy groups and diamines. The number average molecular weight ( $M_n$ ) of the P(DMAEMA-*c*-GMA) copolymers can be regulated by changing the [monomer]/[initiator] ratio. Table 1 shows, with the increase in [monomer]/[initiator] ratio from 100 to 400,  $M_n$  of P(DMAEMA-*c*-GMA) increased from  $8.0 \times 10^3$   $\text{g mol}^{-1}$  to  $2.6 \times 10^4$   $\text{g mol}^{-1}$ , while the polydispersity index (PDI) remains around 1.3.

The chemical structures of the P(DMAEMA-*c*-GMA) copolymers were first studied by  $^1\text{H}$  NMR spectroscopy. Fig. 2(a) shows the  $^{13}\text{C}$  NMR spectrum of the P(DMAEMA-*c*-GMA)2

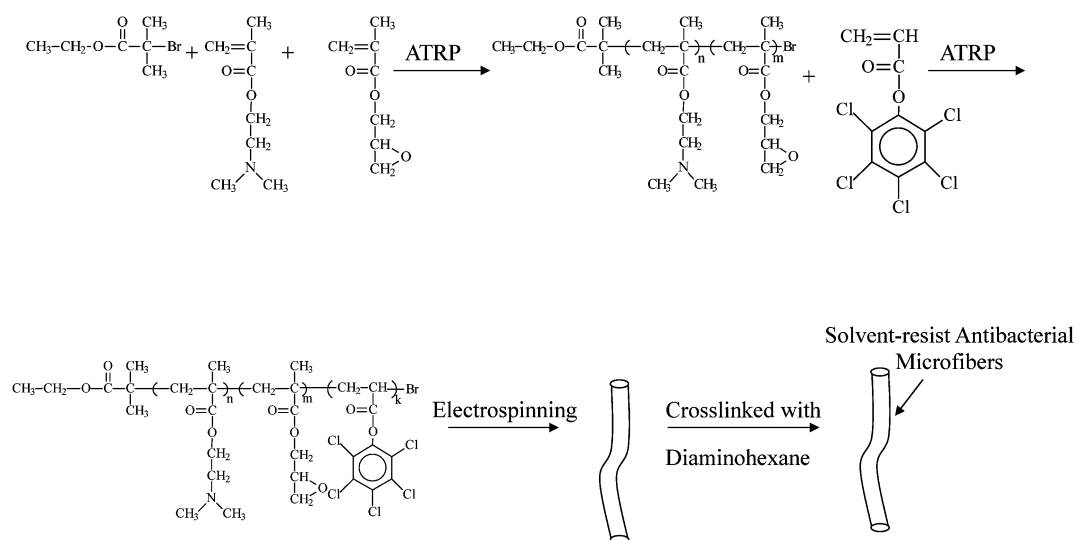
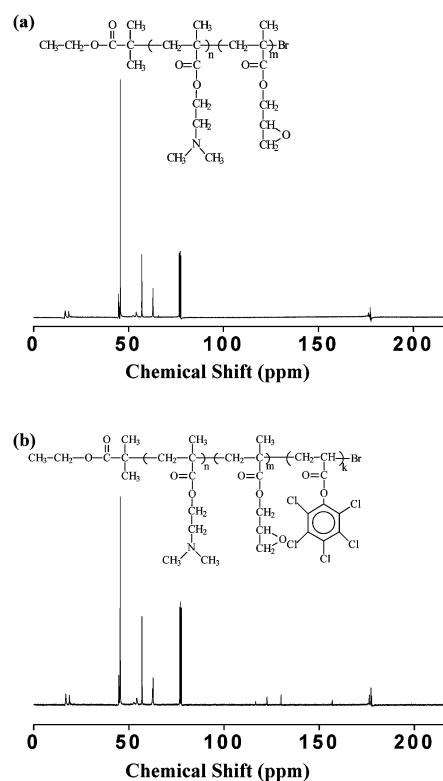


Fig. 1 Schematic illustration of the preparation of P(DMAEMA-*c*-GMA)-*b*-PPCPA microfibers *via* ATRP and electrospinning.

**Table 1** Characterization of P(DMAEMA-*c*-GMA) and P(DMAEMA-*c*-GMA)-*b*-PPCPA polymers

Sample	Monomer/initiator ratio	Polymerization time/h	$M_n/10^3$ g mol <sup>-1</sup>	Polydispersity index (PDI)	GMA content <sup>c</sup> (mol%)	PPCPA content		Repeat units [GMA] : [DMAEMA] : [PCPA]
						GPC <sup>d</sup> (mol%)	NMR <sup>e</sup> (mol%)	
P(DMAEMA- <i>c</i> -GMA)1	90 : 10 : 1 <sup>a</sup>	4	8	1.1	7			
P(DMAEMA- <i>c</i> -GMA)2	190 : 10 : 1	4	17	1.2	6			
P(DMAEMA- <i>c</i> -GMA)3	380 : 20 : 1	6	26	1.3	5			
P(DMAEMA- <i>c</i> -GMA)- <i>b</i> -PPCPA1 <sup>b</sup>	100 : 1	4	21	1.2	6	10	15	8 : 110 : 20
P(DMAEMA- <i>c</i> -GMA)- <i>b</i> -PPCPA2 <sup>b</sup>	100 : 1	8	26	1.3	5	21	26	8 : 110 : 41
P(DMAEMA- <i>c</i> -GMA)- <i>b</i> -PPCPA3 <sup>b</sup>	100 : 1	12	32	1.3	4	28	33	8 : 110 : 58

<sup>a</sup> The molar ratio of [DMAEMA] : [GMA] : [EBB] = 90 : 10 : 1. DMAEMA: (2-dimethylamino)ethyl methacrylate, GMA: glycidyl methacrylate, EBB: ethyl 2-bromoisobutyrate. <sup>b</sup> Using P(DMAEMA-*c*-GMA)2 as the macroinitiator. <sup>c</sup> Deduced from NMR results. <sup>d</sup> Determined from  $(M_n(\text{P(DMAEMA-}c\text{-GMA)}-b\text{-PPCPA)} - M_n(\text{P(DMAEMA-}c\text{-GMA)})) / M_n(\text{P(DMAEMA-}c\text{-GMA)}-b\text{-PPCPA)}$ . <sup>e</sup> Determined from the area ratio of the aromatic carbon at a chemical shift of about 155 ppm and the carbonyl carbon at chemical shifts of about 175 ppm. <sup>f</sup> Calculated from NMR results.



**Fig. 2** 300 MHz <sup>13</sup>C NMR spectra of (a) P(DMAEMA-*c*-GMA)2 polymer in Table 1 ( $M_n = 1.7 \times 10^4$  g mol<sup>-1</sup>, PDI = 1.2) and (b) P(DMAEMA-*c*-GMA)-*b*-PPCPA1 polymer in Table 1 ( $M_n = 2.1 \times 10^4$  g mol<sup>-1</sup>).

copolymer in Table 1 ( $M_n = 1.7 \times 10^4$  g mol<sup>-1</sup>, PDI = 1.2). The chemical shifts at 15–20 ppm are attributable to the methyl carbons (CH<sub>3</sub>) of the 2-bromoisobutyrate initiators, PGMA and PDMAEMA. The chemical shifts in the region of 44–67 ppm are associated with carbons of the main chains of P(DMAEMA-*c*-GMA), the methylidene carbon of glycidyl groups of PGMA, as well as methylidene carbon and *N*-methyl carbons of PDMAEMA. The chemical shifts at about 175 ppm are assigned to the carbonyl carbon of the PGMA and PDMAEMA. The GMA content in the P(DMAEMA-*c*-GMA) copolymer can be calculated from the <sup>13</sup>C NMR spectrum, using the area ratio of the methylidene carbon of the epoxy group at a chemical shift of about 53.4 ppm and carbonyl carbons at a chemical shift of about 175 ppm. The NMR-derived compositions of the copolymers are given in Table 1 (Fig. 1).

The chemical compositions of the P(DMAEMA-*c*-GMA) copolymers were studied by XPS. Fig. 3(a) shows the C 1s core-level spectrum of P(DMAEMA-*c*-GMA)2 in Table 1. The spectrum was curve-fitted with five peak components, having binding energies (BEs) at 284.6 eV for the C–H and C–C species, at 285.6 eV for C–N species, at 286.2 eV for the C–O–C=O species, at 286.6 eV for C–O species of the epoxy group and at about 288.5 eV for the O=C–O species.<sup>23,24</sup> The C–Br species have BEs at about 285.4 eV, which overlaps with that (285.2 eV) of the C–N species. The presence of a Br 3d peak component at the BE of about 69 eV suggests that alkyl bromide groups are well-preserved at the end of the P(DMAEMA-*c*-GMA) (inset of Fig. 3(a)). The bromide content of P(DMAEMA-*c*-GMA)2

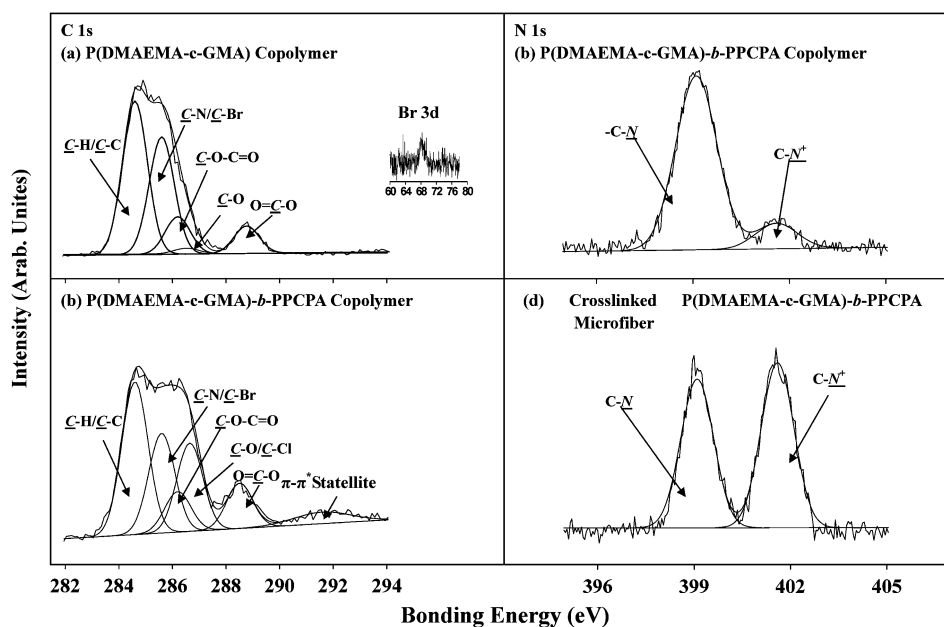


**Fig. 3** XPS wide scan spectra of (a) P(DMAEMA-*c*-GMA)<sub>2</sub> in Table 1 with  $M_n = 1.7 \times 10^4 \text{ g mol}^{-1}$  and of (b) P(DMAEMA-*c*-GMA)-*b*-PPCPA<sub>3</sub> in Table 1 ( $M_n = 3.2 \times 10^4 \text{ g mol}^{-1}$ ). XPS N 1s core-level spectra of (c) P(DMAEMA-*c*-GMA)-*b*-PPCPA<sub>2</sub> copolymer (PPCPA content of 26 mol%) and (d) microfibers from P(DMAEMA-*c*-GMA)-*b*-PPCPA<sub>2</sub>.

is about 0.81‰ (atom concentration), which is very close to the theoretical value of about 0.84‰ (calculated from  $M_n$  of P(DMAEMA-*c*-GMA)<sub>2</sub>). Thus, more than 95% of P(DMAEMA-*c*-GMA) macromolecules were terminated by alkyl bromide groups. The PGMA content in the P(DMAEMA-*c*-GMA) copolymer can also be estimated from the area ratio of the [C–O] species at a BE of about 286.6 eV and [O=C–O] species at a BE of about 288.5 eV. The GMA content in P(DMAEMA-*c*-GMA)<sub>2</sub> in Table 1 is about 9 mol%, which is comparable to that (6 mol%) from NMR results.

Block copolymers of P(DMAEMA-*c*-GMA)-*b*-PPCPA were prepared *via* ATRP of PCPA using P(DMAEMA-*c*-GMA) as macroinitiator. The content of PPCPA in P(DMAEMA-*c*-GMA)-*b*-PPCPA copolymers can be regulated by changing the polymerization time. Table 1 shows, as the polymerization time increase from 4 h to 12 h, the content of PPCPA increase from 10 mol% to 28 mol%. Fig. 2(b) show the <sup>13</sup>C NMR spectrum of the P(DMAEMA-*c*-GMA)-*b*-PPCPA<sub>1</sub> in Table 1. The chemical shifts at 15–20 ppm are attributable to the methyl carbon (CH<sub>3</sub>) of the 2-bromoisobutyrate initiators, PGMA and PDMAEMA. The chemical shifts in the region of 44–67 ppm are associated with main chain carbons of the P(DMAEMA-*c*-GMA)-*b*-PPCPA, the methylidyne carbon of epoxy groups of PGMA, as well as *N*-methyl carbons of PDMAEMA. The presence of the chemical shift at the region of 120 to 155 ppm assigned to the aromatic carbons of the PPCPA block indicates that the P(DMAEMA-*c*-GMA)-*b*-PPCPA have been successfully prepared. The PPCPA content can be calculated from the <sup>13</sup>C NMR spectrum, using the areas of the aromatic carbon at a chemical shift of 155 ppm and the carbonyl carbon at a chemical shift of about 175 ppm. The results are summarized in Table 1. The PPCPA content of P(DMAEMA-*c*-GMA)-*b*-PPCPA copolymers obtained from NMR is slightly higher than those from GPC, which is attributable the difference in

hydrodynamic volume of PPCPA and the PS standards used for GPC measurements. Fig. 3(b) shows the C 1s core-level spectrum of P(DMAEMA-*c*-GMA)-*b*-PPCPA<sub>3</sub> in Table 1. The spectrum was curve-fitted with six peak components, having BEs at 284.6 eV for the C–H and C–C species, at 285.6 eV for C–N and C–Br species, at 286.2 eV for the C–O–C=O species, at 286.6 eV for C–O species and C–Cl species, at about 288.5 eV for the O=C–O species and at 291.9 eV for  $\pi$ - $\pi^*$  shake-up satellite of the aromatic rings of PPCPA.<sup>23,24</sup> The substantial increase in intensity at a BE of 286.6 eV and the presence of peak components at 291.9 eV indicate that P(DMAEMA-*c*-GMA)-*b*-PPCPA block copolymers were successfully prepared. The mechanism of ATRP is based on a rapid dynamic equilibrium between a minute amount of growing radicals and a majority of dormant species.<sup>17,18</sup> Thus, there would be some P(DMAEMA-*c*-GMA), which is not bromo-terminated and cannot initiate ATRP of PCPA, remaining in the resulting P(DMAEMA-*c*-GMA)-*b*-PPCPA polymers. However, due to the minute amount (less than 5%) and the similar  $M_n$  of P(DMAEMA-*c*-GMA) to P(DMAEMA-*c*-GMA)-*b*-PPCPA polymers, it was not observed distinctly in GPC curves.

### 3.2. Electrospinning of P(DMAEMA-*c*-GMA)-*b*-PPCPA block copolymers

Electrospinning is an attractive approach for fabrication of continuous fibers with diameters from micrometer to nanometer scales.<sup>26</sup> Factors such as solution viscosity, solution conductivity, surface tension and electric field intensity markedly influence the morphology of the resulting fibers.<sup>27</sup> In this study, a mixture of THF and DMF (volume ratio = 3 : 2) was used as solvent for electrospinning. Fig. 4(a) shows the scanning electron microscopy (SEM) image of microfibers electrospun from P(DMAEMA-*c*-GMA)-*b*-PPCPA<sub>2</sub> in Table 1 at a concentration

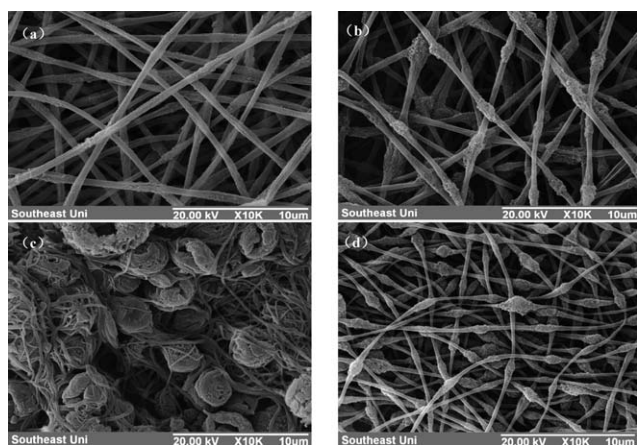


**Fig. 4** SEM surface images of (a) microfibers electrospun from P(DMAEMA-*c*-GMA)-*b*-PPCPA2 in Table 1 at a concentration of about 20 wt%, (b) microfibers from P(DMAEMA-*c*-GMA)-*b*-PPCPA2 in Table 1 with an electrospinning concentration of 15 wt%, (c) microfibers from P(DMAEMA-*c*-GMA)-*b*-PPCPA2 polymer at a concentration of 20 wt% without crosslinking with diamines after immersion in water for 2 h, and (d) crosslinked microfibers from P(DMAEMA-*c*-GMA)-*b*-PPCPA2 after immersion in water and ethanol for 2 h.

of about 20 wt%. The fibers with an average diameter of about 640 nm are well defined. Table 2 summarizes the results of the fibers from electrospinning of P(DMAEMA-*c*-GMA)-*b*-PPCPA polymers at various concentrations. The decrease in concentration of P(DMAEMA-*c*-GMA)-*b*-PPCPA leads to reduction of the size of the microfibers. For P(DMAEMA-*c*-GMA)-*b*-PPCPA2, with the concentration decreasing from 35 wt% to 15 wt%, the average diameters of the microfibers were reduced from 800 nm to 400 nm. Fig. 4(b) shows the microfibers electrospun from P(DMAEMA-*c*-GMA)-*b*-PPCPA2 in Table 1 with an electrospinning concentration of 15 wt%. The average diameter of the microfibers was reduced to 400 nm, and beads on fiber were found. Upon further decreasing the electrospinning concentration of P(DMAEMA-*c*-GMA)-*b*-PPCPA to 5 wt%, no continuous fibers were obtained. The viscosity of the solution for electrospinning is one of the important factors for the formation of the fibers. When the concentration of polymer is lower than a critical point, the viscosity of the solution is not high enough to maintain a stable jet. Thus, beads on fibers or beads were formed. Table 2 also shows that the increase in the content of PPCPA also leads to the increase in size of the resulting microfibers. At an electrospinning concentration of 20 wt%, when

the content of PPCPA increases from 15 mol% (P(DMAEMA-*c*-GMA)-*b*-PPCPA1 polymers in Table 1,  $M_n = 2.1 \times 10^4$  g mol<sup>-1</sup>, repeat unit ratio [GMA] : [DMAEMA] : [PCPA] = 8 : 110 : 20) to 33 mol% (PPCPA-*b*-P(DMAEMA-*c*-GMA)<sub>2</sub> polymers in Table 1,  $M_n = 3.2 \times 10^4$  g mol<sup>-1</sup>, repeat unit ratio [GMA] : [DMAEMA] : [PCPA] = 8 : 110 : 58), the average diameter of the resulting microfibers increases from 320 nm to 680 nm correspondingly.

### 3.3. Crosslinking of the microfibers

Microfibers with crosslinked structure are of great interest because the crosslinking not only improves their mechanical strength but also makes them stable in solvents. Polymers containing epoxy groups can be easily crosslinked by alkyl diamine.<sup>27,28</sup> In this work, the aim to introduce GMA units in the P(DMAEMA-*c*-GMA)-*b*-PPCPA polymer is to generate crosslinking sites for nanofibers. The microfibers of P(DMAEMA-*c*-GMA)-*b*-PPCPA were crosslinked by treatment with 5% hexanediamine solution in petroleum ether for 4 h. The solvent-resistant properties of the microfibers were studied *via* immersion of microfibers in solvent for 1 h. Fig. 4(c) shows the SEM image of the microfibers electrospun from P(DMAEMA-*c*-GMA)-*b*-PPCPA2 polymer (electrospinning with a concentration of about 20 wt%) without treatment of diamines after immersion in water for 2 h. The structure of the microfiber was destroyed. Fig. 4(d) show the SEM image of the crosslinked microfibers after water and ethanol treatment. The nanostructures of the fibers are well preserved. SEM results suggest the crosslinked microfibers are solvent-resistant to common solvents, such as water and ethanol. The crosslinking of the microfibers was also confirmed by the increase in the [N]/[O] ratio. XPS results show that P(DMAEMA-*c*-GMA)-*b*-PPCPA2 polymer has a [N]/[O] ratio of about 0.48, while the [N]/[O] ratio increased to 0.52 in its microfibers after treatment with 1,6-hexanediamine. The increase in the nitrogen content accounts for the reaction between the diamine and epoxy groups leading to a crosslinking structure in the resulting microfibers.

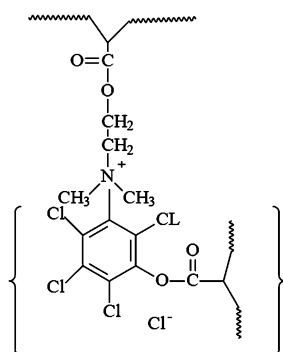
### 3.4. Antibacterial activity of self-quaternized and crosslinked P(DMAEMA-*c*-GMA)-*b*-PPCPA microfibers

The antibacterial activities of the crosslinked P(DMAEMA-*c*-GMA)-*b*-PPCPA microfibers are the main concern in this study. *N*-Alkylated PDMAEMA polymer exhibits good antibacterial effects against gram-positive and gram-negative bacteria.<sup>29,30</sup> The antibacterial activity of *N*-alkylated PDMAEMA is attributed to the formation of quaternary ammonium salts (QASs),

**Table 2** Characterization of PPCPA-*b*-P(DMAEMA-*c*-GMA) microfibers

Concentration	Diameter of microfibers <sup>b</sup> /nm		
	PPCPA- <i>b</i> -P(DMAEMA- <i>c</i> -GMA)1	PPCPA- <i>b</i> -P(DMAEMA- <i>c</i> -GMA)2	PPCPA- <i>b</i> -P(DMAEMA- <i>c</i> -GMA)3
15 (wt%) <sup>a</sup>	300 ± 62	400 ± 60	420 ± 80
20 (wt%) <sup>a</sup>	320 ± 83	640 ± 75	680 ± 93
35 (wt%) <sup>a</sup>	430 ± 101	800 ± 86	1260 ± 74

<sup>a</sup> Electrospinning was carried out using mixed THF-DMF (3 : 2 in volume) as solvent, an electrical potential of 10 kV and a needle with an inner diameter of about 0.6 mm. The distance between the tip of the needle and the grounded collector was fixed at about 20 cm. <sup>b</sup> Average diameter of 50 microfibers was determined from SEM images.



**Scheme 1** Schematic illustration of the self-quaternized P(DMAEMA-*c*-GMA)-*b*-PPCPA.

which were generated *via* *N*-alkylation of PDMAEMA by alkyl bromide with 6 to 12 carbon units.<sup>10,11</sup>

For P(DMAEMA-*c*-GMA)-*b*-PPCPA, QASs (N<sup>+</sup>) were generated *via* *N*-alkylation of tertiary alkylamine groups of the PDMAEMA blocks by the chloro-aromatic compounds of the PPCPA block (self-quaternization of P(DMAEMA-*c*-GMA)-*b*-PPCPA). The formation of the QASs *via* self-quaternization of the P(DMAEMA-*c*-GMA)-*b*-PPCPA polymers is schematically shown in Scheme 1. Fig. 3(c) show the N 1s core-level spectrum of the P(DMAEMA-*c*-GMA)-*b*-PPCPA2 ( $M_n = 2.6 \times 10^4$  g/mol, PPCPA content of 26 mol%). The peak components at BE of 399.1 eV and 401.9 eV are attributable to =N- and N<sup>+</sup> species respectively.<sup>23,24</sup> The appearance of N<sup>+</sup> species confirmed the self-quaternization of P(DMAEMA-*c*-GMA)-*b*-PPCPA. Fig. 3(d) shows the N 1s core-level spectrum of the crosslinked microfibers from P(DMAEMA-*c*-GMA)-*b*-PPCPA2 copolymer. The [N<sup>+</sup>]/[=N-] ratio of the microfibers is about 1.1, which is much higher than that (0.2) of its original copolymer (Fig. 3(c)). The XPS results indicate the process of electrospinning increases the degree of self-quaternization of P(DMAEMA-*c*-GMA)-*b*-PPCPA. Note that if one PCPA quaternized with one DMAEMA unit, the theoretical [N<sup>+</sup>]/[=N-] ratio would be about 0.54. A higher [N<sup>+</sup>]/[=N-] ratio in P(DMAEMA-*c*-GMA)-*b*-PPCPA microfibers can be accounted for the fact that one PCPA units can quaternize more than one tertiary alkylamine group in the resulting crosslinked microfibers.

The antimicrobial assays were first conducted with suspensions of gram-positive bacteria (*S. aureus*), containing  $1 \times 10^5$  cells ml<sup>-1</sup>. Fig. 5 shows the time-dependent viable cell concentration after 50 mg of the self-quaternized P(DMAEMA-*c*-GMA)-*b*-PPCPA microfibers and PPCPA polymers were placed in contact with 50 ml of the bacterial suspension. The PPCPA polymers have poor solubility in common solvents and are difficult to prepare into microfibers *via* electrospinning. Thus, PPCPA polymer powders were used for the antibacterial assays. About 99.0% of *S. aureus* cells were killed after coming into contact with PPCPA polymers in 60 min. The chloro-aromatic compounds of PPCPA are highly hydrophobic. When *S. aureus* cells come into contact with PPCPA, the hydrophobic interaction would lead to swelling of the membrane bilayer, thus affecting the function of the membrane and membrane-embedded proteins.<sup>31</sup> For crosslinked microfibers electrospun from P(DMAEMA-*c*-GMA)-*b*-PPCPA1 polymer ( $M_n = 2.1 \times 10^4$  g mol<sup>-1</sup>, [GMA] : [DMAEMA] : [PPCPA] = 8 : 110 : 20, average diameter = 300

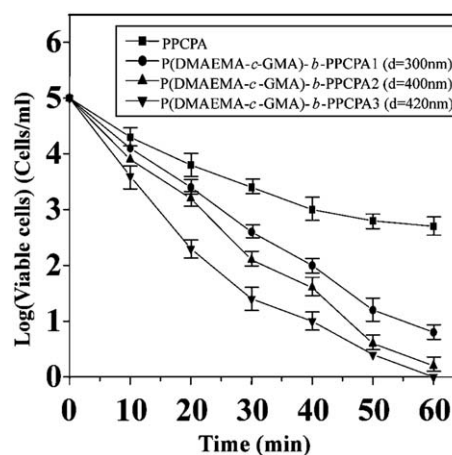


**Fig. 5** Antibacterial efficacy of 50 mg of PPCPA polymers and self-quaternized microfibers electrospun from P(DMAEMA-*c*-GMA)-*b*-PPCPA copolymers in contact with 50 ml of *S. aureus* suspension ( $10^5$  CFU ml<sup>-1</sup>).

nm), the number decreases by 3 orders of magnitude in 30 min. Thus, antibacterial efficiencies of 99.9% were obtained. It is well known that the cell surfaces of bacteria are negatively charged.<sup>10</sup> When cells come into contact with P(DMAEMA-*c*-GMA)-*b*-PPCPA microfibers having QASs on the surface, the normal function of the cell membrane is disrupted due to the electrostatic interaction.<sup>11</sup> Combination of the hydrophobic interaction of PPCPA block and electrostatic interaction of QASs generated from the self-quaternization of P(DMAEMA-*c*-GMA)-*b*-PPCPA resulted in microfibers exhibiting high antibacterial efficiency. Fig. 5 also shows the antibacterial assay results of microfibers electrospun from P(DMAEMA-*c*-GMA)-*b*-PPCPA2 ( $M_n = 2.6 \times 10^4$  g mol<sup>-1</sup>, [GMA] : [DMAEMA] : [PPCPA] = 8 : 110 : 41, average diameter = 400 nm) and microfiber from P(DMAEMA-*c*-GMA)-*b*-PPCPA3 in Table 1 ( $M_n = 3.6 \times 10^4$  g mol<sup>-1</sup>, [GMA] : [DMAEMA] : [PPCPA] = 8 : 110 : 57, average diameter = 420 nm). Microfibers from P(DMAEMA-*c*-GMA)-*b*-PPCPA3 exhibit higher antibacterial efficiency than those from P(DMAEMA-*c*-GMA)-*b*-PPCPA1 and from P(DMAEMA-*c*-GMA)-*b*-PPCPA2. The higher antibacterial efficiency of microfibers from P(DMAEMA-*c*-GMA)-*b*-PPCPA3 is attributable to the high PPCPA content. The higher PPCPA content in P(DMAEMA-*c*-GMA)-*b*-PPCPA would lead to a stronger hydrophobic interaction and a higher QASs concentration in the resulting microfibers. However, the content of PPCPA can not increase more than 50 mol% due to the poor solubility and the difficulty in electrospinning of the resulting copolymers.

Antibacterial assays were also carried out with suspensions of gram-negative bacteria, *E. coli*, containing  $1 \times 10^5$  cells ml<sup>-1</sup>. For PPCPA polymers, about 96% of *E. coli* were killed after coming into contact with PPCPA polymers in 60 min. All microfibers from P(DMAEMA-*c*-GMA)-*b*-PPCPA polymer exhibit higher antibacterial efficiency than that of PPCPA. For microfibers from P(DMAEMA-*c*-GMA)-*b*-PPCPA1 ( $M_n = 2.1 \times 10^4$  g mol<sup>-1</sup>, [GMA] : [DMAEMA] : [PPCPA] = 8 : 110 : 20, average diameter = 300 nm), the viable cell number decreases by 2.5 order of magnitude in 30 min. Thus, bacterial efficiencies of 99.7% were obtained (Fig. 6). Fig. 6 also indicate that increasing

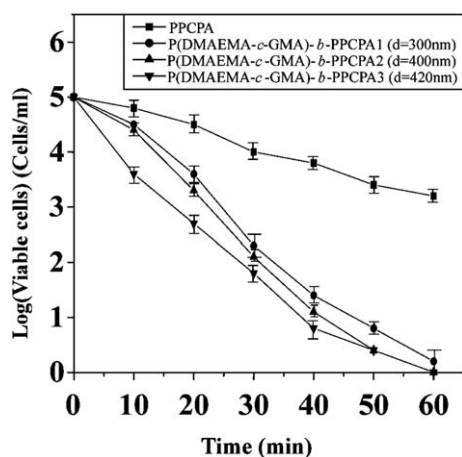


**Fig. 6** Antibacterial efficacy of 50 mg of PPCPA polymers and self-quaternized microfibrers electrospun from P(DMAEMA-*c*-GMA)-*b*-PPCPA copolymers in contact with 50 ml of *E. coli* suspension ( $10^5$  CFU ml<sup>-1</sup>).

PPCPA content in P(DMAEMA-*c*-GMA)-*b*-PPCPA polymer leads to an improved antibacterial efficiency for *E. coli* in the resulting fibers.

The permanence of the antibacterial efficiency of the cross-linked P(DMAEMA-*c*-GMA)-*b*-PPCPA microfibrers is another main concern in this study. The crosslinked P(DMAEMA-*c*-GMA)-*b*-PPCPA microfibrers maintain almost constant antibacterial efficacy for *E. coli* and *S. aureus* after five batches of repeated applications. Polymer with QAS groups generated from *N*-alkylation of tertiary alkylamine groups and alkyl halide exhibit good antibacterial activities. However, the slow leaching of the active groups in repeated applications will lead to the loss of antibacterial efficacy.<sup>3233</sup> In the present work, the antibacterial activity of crosslinked P(DMAEMA-*c*-GMA)-*b*-PPCPA microfibrers results from hydrophobic interactions of PPCPA blocks and electrostatic interactions of QASs, which were generated from self-quaternization of P(DMAEMA-*c*-GMA)-*b*-PPCPA. PPCPA is very stable in common solvents, thus, the slow loss of active groups was largely prevented. This result is also confirmed by XPS analysis. The [N<sup>+</sup>]/[=N-] ratio and [Cl]/[C] ratio of P(DMAEMA-*c*-GMA)-*b*-PPCPA microfibrers remain almost constant after five batches of antibacterial assay.

#### 4. Conclusion

Well-defined block copolymers of poly[(2-dimethylamino)ethyl methacrylate]-*co*-(glycidyl methacrylate)] (P(DMAEMA-*c*-GMA)) and poly(pentachlorophenyl acrylate) (PPCPA) (P(DMAEMA-*c*-GMA)-*b*-PPCPA) were synthesized *via* consecutive atom transfer radical polymerizations (ATRP). Electrospinning of P(DMAEMA-*c*-GMA)-*b*-PPCPAP and subsequent treatment with diamine gave rise to crosslinked microfibrers with diameters in the range of 300 nm to 1.3  $\mu$ m. The microfibrers are solvent-resistant to water and common solvents. Combination of the hydrophobic interaction of the PPCPA blocks and electrostatic interaction of quaternary ammonium salts (QASs) generated from the *N*-alkylation between the chloro-aromatic compounds of the PPCPA and tertiary amine groups of DMAEMA resulted in cross-linked microfibrers exhibiting good antibacterial activities

to *E. coli* and *S. aureus*. Increasing the PPCPA content of microfibrers can improve the antibacterial efficiency. However, the content of PPCPA cannot increase more than 50 mol% due to the poor solubility and the difficulty in electrospinning of the resulting copolymers. The permanence of the antibacterial activity of P(DMAEMA-*c*-GMA)-*b*-PPCPA microfibrers was demonstrated by repeated antibacterial application. In comparison to other QASs containing polymers, which were prepared by *N*-alkylation of the tertiary amine groups by alkyl halides, the QASs of the microfibrers are formed from the self-quaternization of P(DMAEMA-*c*-GMA)-*b*-PPCPA. Thus, the loss of the antibacterial activity of the material due to slow leaching of the small molecules is largely prevented.

#### Acknowledgements

This work was supported by Southeast University foundations of 4007041012 and 4007041023. This work was also funded by State Key Laboratory for Modification of Chemical Fibers and Polymer Materials, Donghua University, China. We are grateful to Mr Zhao Junpeng and Prof. Kang En-Tang for the XPS characterization.

#### References

- 1 C. Burger, B. S. Hsiao and B. Chu, *Annu. Rev. Mater. Res.*, 2006, **36**, 333–368.
- 2 S. Ramakrishna, K. Fujihara, W. E. Teo, T. Yong, and R. Ramaseshan, *Mater. Today*, 2006, **9**(3), 40–50.
- 3 B. Gottenbos, H. C. van der Mei, F. Flatter, P. Nieuwenhuis and H. J. Busscher, *Biomaterials*, 2002, **23**, 1417–1426.
- 4 A. Melaiye, Z. H. Sun, K. Hindi, A. Milsted, D. Ely, D. H. Reneker, C. A. Tessier and W. J. Youngs, *J. Am. Chem. Soc.*, 2005, **127**, 2285–2291.
- 5 X. Y. Xu, Q. B. Yang, Y. Z. Wang, H. Yu, X. Chen and X. B. Jing, *Eur. Polym. J.*, 2006, **42**, 2081–2087.
- 6 M. Tsukada, T. Arai, G. M. Colonna, A. Boschi and G. Freddi, *J. Appl. Polym.*, 2003, **89**, 638–644.
- 7 K. H. Hong, *Polym. Eng. Sci.*, 2007, 43–49.
- 8 M. Jin, X. Zhang, S. Nishimoto, Z. Liu, D. A. Tryk, A. V. Emeline, T. Murakami and A. Fujishima, *J. Phys. Chem. C*, 2007, **111**, 658–665.
- 9 K. de Arruda Alerda, A. A. A. de Queiroz, O. Z. Higa, G. A. Abraham and J. S. Roman, *J. Biomed. Mater. Res., Part A*, 2004, **68**, 473–478.
- 10 T. Tashiro, *Macromol. Mater. Eng.*, 2001, **286**, 63–87.
- 11 A. M. Klibanov, *J. Mater. Chem.*, 2007, **17**, 2479–2482.
- 12 L. Fan, Y. Du, B. Zhang, J. Yang, J. Zhou and J. F. Kennedy, *Carbohydr. Polym.*, 2006, **65**, 447–452.
- 13 M. Ignatova, K. Starbova, N. Markova, N. Manolova and I. Rashkov, *Carbohydr. Res.*, 2006, **341**, 2098–2107.
- 14 M. Ignatova, N. Manolova and I. Rashkov, *Eur. Polym. J.*, 2007, **43**, 1112–1122.
- 15 F. X. Hu, K. G. Neoh and E. T. Kang, *Biotechnol. Bioeng.*, 2005, **89**(4), 474–484.
- 16 T. E. Patten and K. Matyjaszewski, *Adv. Mater.*, 1998, **10**, 901–915.
- 17 V. Coessens, T. Pintauer and K. Matyjaszewski, *Prog. Polym. Sci.*, 2001, **26**, 337–377.
- 18 K. Matyjaszewski and J. Xia, *Chem. Rev.*, 2001, **101**, 2921–2290.
- 19 J. Pyun, T. Kowalewski and K. Matyjaszewski, *Macromol. Rapid Commun.*, 2003, **24**(18), 1043–1059.
- 20 S. Edmondson, V. L. Osborne and W. T. S. Huck, *Chem. Soc. Rev.*, 2004, **33**(1), 14–22.
- 21 E. R. Freiter, Chlorophenol, *Kirk-Othmer Encyclopedia of Chemical Technology*, 3rd edn, John Wiley and Sons, N.Y., 1980, vol 5, pp. 864–872.
- 22 M. Gavrilescu, *Eng. Life Sci.*, 2005, **5**(6), 497–526.
- 23 G. Beamsom and D. Briggs, *High Resolution XPS of Organic Polymers The scienta ESCA 300 Databse*, John Wiley & Son, Chichester, England, 1992, p. 274.

- 24 *Handbook of X-ray Photoelectron Spectroscopy*, ed. G. E. Muilenberg, Perkin-Elmer, Eden Prairie, MN, 1978, p. 94.
- 25 A. Greiner and J. H. Wendorff, *Angew. Chem., Int. Ed.*, 2007, **46**, 5670–5703.
- 26 S. V. Fridrick, J. H. Yu, M. P. Brenner and G. C. Rutledge, *Phys. Rev. Lett.*, 2003, **90**(14), 144502–1.
- 27 V. Rebizant, V. Abetz, F. Tournilhac, F. Court and L. Leibler, *Macromolecules*, 2003, **36**(26), 9889–9896.
- 28 L. Matejka, O. Dukh, B. Meissner, D. Hlavata, J. Brus and A. Strachota, *Macromolecules*, 2003, **36**(21), 7977–7985.
- 29 J. Y. Huang, H. Murata, R. R. Koepsel, A. J. Russell and K. Matyjaszewski, *Biomacromolecules*, 2007, **8**(5), 1396–1399.
- 30 E. Yancheva, D. Paneva, V. Maximova, L. Mespouille, P. Dubois, N. Manolova and I. Rashkov, *Biomacromolecules*, 2007, **8**(3), 976–984.
- 31 J. Sikkema, J. A. M. de Bont and B. Poolman, *J. Biol. Chem.*, 1994, 8022–8028.
- 32 Y. Chen, S. D. Worley, T. S. Huang, J. Weese, J. Kim, C. I. Wei and J. F. Williams, *J. Appl. Polym. Sci.*, 2004, **92**, 368–372.
- 33 L. Cen, K. G. Neoh and E. T. Kang, *J. Biomed. Mater. Res., Part A*, 2004, **71**(A), 70–80.